

Electronic Supplementary Information

Lysosome-Targeting Ratiometric Fluorescent pH Probes based on Long-Wavelength BODIPY

Mengliang Zhu, Peipei Xing, Yabin Zhou, Lei Gong, Jinghui Zhang, Dongdong Qi,
Yongzhong Bian, Hongwu Du and Jianzhuang Jiang

Content

- 1 Chemicals and Instruments, page S3.
- 2 Cell culture and confocal microscopy study, pages S4-5.
- 3 Synthesis and Characterization, pages S6-8.
- 4 Scheme S1, synthesis of probes **A** and **B**, page S9.
- 5 Figs. S1-S5, ¹H NMR, ¹H-¹H COSY, ¹³C NMR and MALDI-TOF MS of probes **A** and **B**, pages S10-14.
- 6 Table S1, photophysical properties of probes **A** and **B** in different solvents, pages S15.
- 7 Fig. S6, absorption and emission spectra of probes **A** and **B** in different solvents, page S16.
- 8 Fig. S7, Optical responses of probe **B** (5 μM) in THF/H₂O (1:1, v/v) at different pH values, page S17.
- 9 Fig. S8, ¹H NMR spectra of probes **A** and **B** after addition of CF₃COOD, page S18.
- 10 Theoretical calculations, Table S2, Fig. S9, calculated HOMO and LUMO energies of the probes and morpholine moiety before and after protonation, pages S19-20.
- 11 Scheme S2, the pH-modulated ICT mechanism for probe **B**, page S21.

- 12 Figs. S10-11, the correlation scatter and intensity profiles of probes and LysoTracker™ Blue DND-22, page S22.
- 13 Fig. S12, cell viability estimated by a MTT assay versus incubation in different concentrations of probes **A** and **B**, page S23.
- 14 Fig. S13, fluorescence images of A549 cells incubated with probe **B** under various pH conditions, page S24.
- 15 References, page S25.

Chemicals and instruments.

Column chromatography was carried out on silica gel (200-300 mesh, Qingdao Ocean Chemicals) with the indicated eluents. Toluene was freshly distilled from Na under nitrogen. All other reagents and solvents were used as received. 4,4-difluoro-8-(4-hydroxyphenyl)-1,3,5,7-tetramethyl-4-bora-3a,4a-diaza-s-indacene (**1**)¹ was prepared according to the published procedures.

¹H NMR spectra were recorded on a Bruker DPX 400 MHz spectrometer in CDCl₃ or DMSO-d₆ and the chemical shifts were reported relative to internal SiMe₄. MALDI-TOF mass spectra were measured on a Bruker Microflex™ LRF spectrometer with dithranol as the matrix. Elemental analyses were performed on an Elementar Vario MICRO CUBE elemental analyzer. Electronic absorption spectra were recorded on a Lambda U-750 spectrophotometer. Steady-state fluorescence spectroscopic studies were performed on a Hitachi F4500 fluorophotometer. The slit width was 10 nm for excitation and emission. The photon multiplier voltage was 700 V.

Cell culture and confocal microscopy study.

A549 cells were cultured in DMEM supplemented with 10% (v/v) FBS, 100 U/mL penicillin and 100 µg/mL streptomycin in an atmosphere of 5% CO₂ and 95% air at 37 °C. Then the cells were incubated for 24 h prior to the imaging experiments. Stock solutions of probe **A** and **B** (1.0 mM) were prepared in centrifuge tubes with DMSO, each working solution (5 µM) was prepared in a centrifuge tube with the corresponding stock solution (50 µL) and DMEM culture medium (5 mL).

Intracellular pH calibration of A549 cells. Cells were treated with probes **A** or **B** (5 µM) for 15 min, and then incubated at 37 °C for 15 min in high K⁺ buffer of various pH values (pH 3.0-6.0) in the presence of 10 µM nigericin and 5 µM monensin. Fluorescence imaging experiments were performed at 37 °C on a Nikon A1RSi+ confocal laser scanning microscope with live cell imaging system and excitation at 488 nm through 100× oil immersion objective lens; fluorescence emissions were collected through the channels of 515-565 nm (Green channel) and 650-700 nm (Red channel) for probe **A**, 515-565 nm (Green channel) and 675-725 nm (Deep red channel) for probe **B**. The ratio of the average fluorescence intensities from the two channels $R (I_{green}/I_{red})$ was estimated using Image pro-plus (Universal Imaging Corp.) software.

Co-localization fluorescence imaging. In this experiment, A549 cells were incubated with probes **A** or **B** (5.0 µM) at 37 °C for 15 min, washed three times with PBS (pH 7.4), and then incubated with LysoTracker™ Blue DND-22 (100 nM) for another 15 min. Before fluorescence imaging, the adherent cells were further washed three times with PBS (pH 7.4) to remove the excess dyes. Fluorescence imaging experiments were performed on

a Nikon A1RSi+ confocal laser scanning microscope with excitations at 405 nm (for DND-22), 561 nm (for probe **A**) and 640 nm (for probe **B**) through 100× oil immersion objective lens; four color channels were used for these experiments: red fluorescence channel (650-700 nm) for probe **A**, deep red/infrared channel (675-725 nm) for probe **B**, and blue channel (425-475 nm) for LysoTracker™ Blue DND-22, respectively. The background fluorescence was zeroed by adjusting the voltage of the photomultiplier tube.

Cell cytotoxicity assays. Probes **A** or **B** were first dissolved in DMSO to give 1 mM solution, which was diluted to appropriate concentration (2.5 μM, 5 μM, 10 μM, 20 μM) with DMEM containing 0.1% Cremophor EL (v/v). A549 cells were cultured in DMEM supplemented with 10% FBS and then seeded into a 96-well plate. After cultured in an incubator for 12 h at 37 °C under 5% CO₂, A549 cells were incubated with probes **A** or **B** (100 μL/well) at concentrations of 2.5-20 μM. For 15 min later, the medium was exchanged with fresh DMEM and the cells were cultured in an incubator at 37 °C under 5% CO₂ for another 24 h before cell viability was measured using the methyl thiazolyl tetrazolium (MTT) assay. The medium was exchanged to 50 μL (5 mg/mL) MTT solution each well followed by incubation for 4 h. The MTT solution was carefully removed and DMSO (150 μL) was added each well. A Tecan Sunrise™ microplate reader was used to measure at OD490 nm. An untreated cell population under the same experimental conditions was used as the reference point to establish 100% cell viability.

Synthesis and Characterization.

3-[4-N,N-dimethylaminophenyl]ethenyl]-4,4-difluoro-8-(4-hydroxyphenyl)-1,3,5,7-tetramethyl-4-bora-3a,4a-diaza-s-indacene (2)

Compound **1** (112 mg, 0.33 mmol) and 4-(N,N-dimethylamino)benzaldehyde (49 mg, 0.33 mmol) were added to a mixture of toluene (20 mL), glacial acetic acid (0.25 mL) and piperidine (0.30 mL). The mixture was stirred and heated under reflux for 72 h. Any water formed during the reaction was removed by a Dean-Stark apparatus. The crude product was concentrated under vacuum, then purified by silica gel column chromatography using EtOAc/hexane = 1:3 as the eluant. The second blue colored fraction was collected and the solvent was removed under reduced pressure to yield **2** (17 mg, 11 %). ¹H NMR (DMSO, 400 MHz, 293K): δ 9.80 (s, 1H, -OH), 7.47 (d, J = 12.0 Hz, 2H, N(CH₃)₂-Ph-H), 7.44 (d, J = 16.0 Hz, 1H, ene-H), 7.24 (d, J = 16.0 Hz, 1H, ene-H), 7.13 (d, J = 8.0 Hz, 2H, BDP-Ph-H), 6.92 (d, J = 8.0 Hz, 2H, BDP-Ph-H), 6.89 (s, 1H, BDP-α-H), 6.78 (d, J = 12.0 Hz, 2H, N(CH₃)₂-Ph-H), 6.11 (s, 1H, BDP-α-H), 3.00 (s, 6H, N-CH₃), 2.45 (s, 3H, -CH₃), 1.48 (s, 3H, -CH₃), 1.42 (s, 3H, -CH₃). ¹³C NMR (DMSO, 400 MHz, 293K): δ 158.0, 154.1, 151.6, 151.2, 142.7, 140.1, 139.6, 138.4, 132.8, 129.3, 128.9, 124.6, 123.6, 120.3, 118.0, 115.9, 112.8, 112.2, 79.2, 14.5, 14.2, 14.0. MALDI-TOF-MS: m/z Calcd for C₂₈H₂₈BF₂N₃O (M⁺) 471.2; Found 471.8. Anal. Calcd for C₂₈H₂₈BF₂N₃O: C, 71.35; H, 5.99; N, 8.91. Found: C, 71.53; H, 6.04; N, 8.93.

3,5-bis[4-N,N-dimethylaminophenyl]ethenyl]-8-(4-hydroxyphenyl)-1,7-dimethyl-4,4-difluoro-4-bora-3a,4a-diaza-s-indacene (3)

Compound **1** (112 mg, 0.33 mmol) and 4-(N,N-dimethylamino)benzaldehyde (98 mg, 0.66 mmol) were added to a mixture of toluene (20 mL), glacial acetic acid (0.50 mL) and piperidine (0.60 mL). The mixture was stirred and heated under reflux for 72 h. Any water formed during the reaction was removed by a Dean-Stark apparatus. The crude product

was concentrated under vacuum, then purified by silica gel column chromatography using EtOAc/hexane = 1:3 as the eluant. The third green colored fraction was collected and the solvent was removed under reduced pressure to yield **3** (30 mg, 15 %). ¹H NMR (DMSO-*d*₆, 400 MHz, 293K): δ 9.79 (s, 1H, -OH), 7.46 (d, J = 16.0 Hz, 4H, N(CH₃)₂-Ph-H), 7.41 (d, J = 12.0 Hz, 2H, ene-H), 7.30 (d, J = 12.0 Hz, 2H, ene-H), 7.16 (d, J = 8.0 Hz, 2H, BDP-Ph-H), 6.93 (d, J = 8.0 Hz, 2H, BDP-Ph-H), 6.86 (s, 2H, BDP-α-H), 6.79 (d, J = 12.0 Hz, 4H, N(CH₃)₂-Ph-H), 3.00 (s, 12H, N-CH₃), 1.48 (s, 6H, -CH₃). ¹³C NMR (DMSO-*d*₆, 400 MHz, 293K): δ 158.0, 152.0, 151.0, 149.5, 140.7, 136.9, 136.3, 129.7, 128.9, 128.7, 128.2, 125.3, 124.0, 117.5, 115.9, 113.4, 112.2, 67.1, 54.9, 35.8, 30.8, 25.1, 21.1, 14.4. MALDI-TOF-MS: m/z Calcd for C₃₇H₃₇BF₂N₄O (M⁺) 602.3; Found 602.2. Anal. Calcd for C₃₇H₃₇BF₂N₄O: C, 73.76; H, 6.19; N, 9.30. Found: C, 73.86; H, 6.13; N, 9.27.

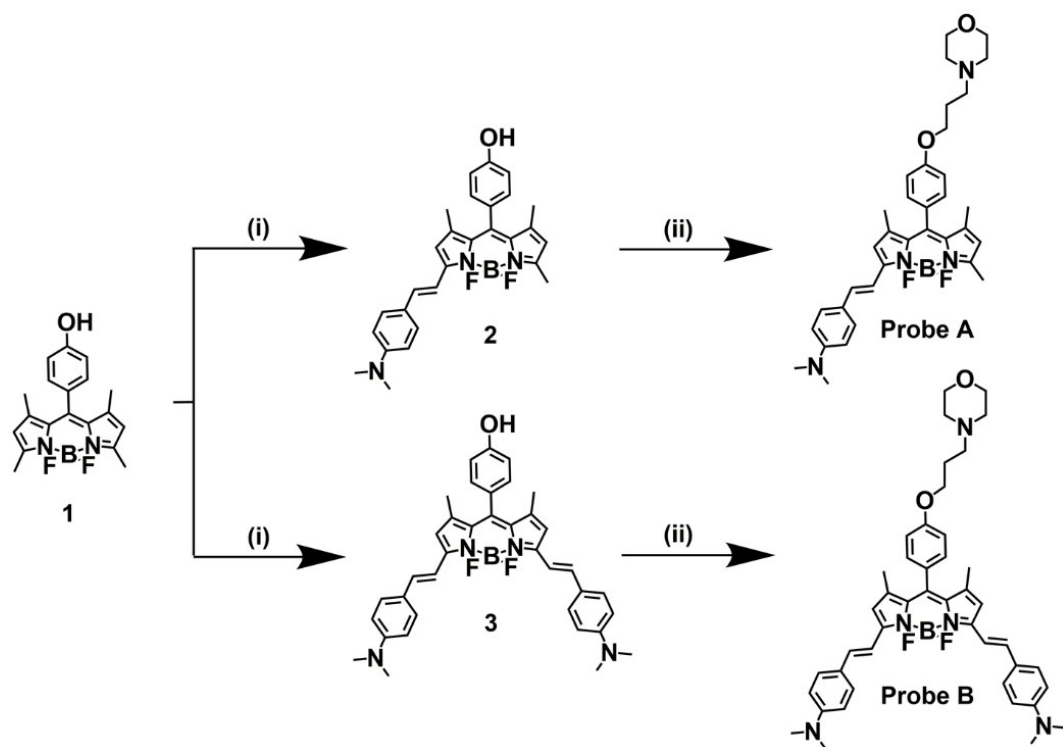
3-[4-N,N-dimethylaminophenyl]ethenyl]-4,4-difluoro-8-[4-(3-morpholinopropoxy)-phenyl]-1,3,5,7-tetramethyl-4-bora-3a,4a-diaza-s-indacene (A)

Compound **2** (20.0 mg, 0.042 mmol), N-(3-chloropropyl)morpholine (10 μL, 0.064 mmol) and anhydrous potassium carbonate (30.0 mg, 0.22 mmol) were added to acetone (25 mL). The mixture was stirred at 50 °C for 48 h and tracked with TLC. Then the mixture was cooled to room temperature, filtered and washed with sufficient amount of acetone. After removal of the solvent under vacuum, the crude product was dissolved in CH₂Cl₂ and washed with H₂O. The organic layer was dried with anhydrous sodium sulfate, and the crude product was purified by silica gel column chromatography using CH₂Cl₂/C₂H₅OH = 100:1 as the eluant to yield **Probe A** (7.5 mg, 30 %). ¹H NMR (CDCl₃, 400 MHz, 293K): δ 7.50 (d, J = 8.0 Hz, 2H, N(CH₃)₂-Ph-H), 7.48 (d, J = 12.0 Hz, 1H, ene-H), 7.21 (d, J = 12.0 Hz, 1H, ene-H), 7.18 (d, J = 8.0 Hz, 2H, BDP-Ph-H), 7.00 (d, J = 8.0 Hz, 2H, BDP-Ph-H), 6.68 (d, J = 8.0 Hz, 2H, N(CH₃)₂-Ph-H), 6.59 (s, 1H, BDP-α-H), 5.96 (s, 1H, BDP-α-H), 4.08 (t, J = 6.0 Hz, 2H,

-CH₂), 3.74 (t, J = 6.0 Hz, 4H, morpholine-CH₂), 3.02 (s, 6H, N-CH₃), 2.58 (t, J = 6.0 Hz, 2H, -CH₂), 2.58 (s, 3H, -CH₃), 2.49 (t, J = 6.0 Hz, 4H, morpholine-CH₂), 2.02 (m, 2H, -CH₂), 1.48 (s, 3H, -CH₃), 1.43 (s, 3H, -CH₃). ¹³C NMR (CDCl₃, 400 MHz, 293K): δ 159.6, 154.8, 153.0, 151.2, 141.0, 139.2, 137.8, 133.6, 131.8, 129.8, 129.4, 127.6, 124.9, 120.5, 117.7, 115.1, 114.6, 112.2, 67.2, 66.5, 55.8, 54.0 40.4, 26.7, 22.8, 15.1, 14.7, 14.6, 14.3. MALDI-TOF-MS: m/z Calcd for C₃₅H₄₁BF₂N₄O₂ (M⁺) 598.3; Found 598.6. Anal. Calcd for C₃₅H₄₁BF₂N₄O₂: C, 70.23; H, 6.90; N, 9.36. Found: C, 70.31; H, 6.94; N, 9.30.

3,5-bis[(4-N,N-dimethylaminophenyl)ethenyl]-8-[4-(3-morpholinopropoxy)phenyl]-1,7-dimethyl-4,4-difluoro-4-bora-3a,4a-diaza-sindacene (B)

Probe B was synthesized by compound **3** (25.3 mg, 0.042 mmol) and N-(3-chloropropyl)morpholine (10 μL, 0.064 mmol) using a similar procedure to **Probe A**. The crude product was purified by silica gel column chromatography using CH₂Cl₂/C₂H₅OH = 100:2 as the eluant to yield **Probe B** (18 mg, 60 %). ¹H NMR (CDCl₃, 400 MHz, 293K): δ 7.58 (d, J = 12.0 Hz, 2H, ene-H), 7.50 (d, J = 16.0 Hz, 4H, N(CH₃)₂-Ph-H), 7.20 (d, J = 8.0 Hz, 2H, BDP-Ph-H), 7.17 (d, J = 12.0 Hz, 2H, ene-H), 7.00 (d, J = 8.0 Hz, 2H, BDP-Ph-H), 6.72 (d, J = 12.0 Hz, 4H, N(CH₃)₂-Ph-H), 6.59 (s, 2H, BDP-α-H), 4.09 (t, J = 6.0 Hz, 2H, -CH₂), 3.75 (t, J = 6.0 Hz, 4H, morpholine-CH₂), 3.03 (s, 12H, N-CH₃), 2.57 (t, J = 8.0 Hz, 2H, -CH₂), 2.50 (t, J = 6.0 Hz, 4H, morpholine-CH₂), 2.03 (m, 2H, -CH₂), 1.48 (s, 6H, -CH₃). ¹³C NMR (CDCl₃, 400 MHz, 293K): δ 159.5, 152.9, 151.0, 141.1, 136.6, 136.3, 133.5, 130.1, 129.2, 127.9, 125.4, 117.3, 115.2, 115.0, 112.3, 67.2, 66.5, 55.8, 54.0 40.4, 26.2, 15.0. MALDI-TOF-MS: m/z Calcd for C₄₄H₅₀BF₂N₅O₂ (M⁺) 729.4; Found 729.9. Anal. Calcd for C₄₄H₅₀BF₂N₅O₂: C, 72.42; H, 6.91; N, 9.60. Found: C, 72.55; H, 6.94; N, 9.55.



Scheme S1 Synthesis of probes **A** and **B**: (i): 4-(*N,N*-dimethylamino)benzaldehyde, Piperidine, AcOH, PhMe, 115 °C, reflux; (ii): *N*-(3-chloropropyl)morpholine, K₂CO₃, Acetone, 55 °C, reflux.

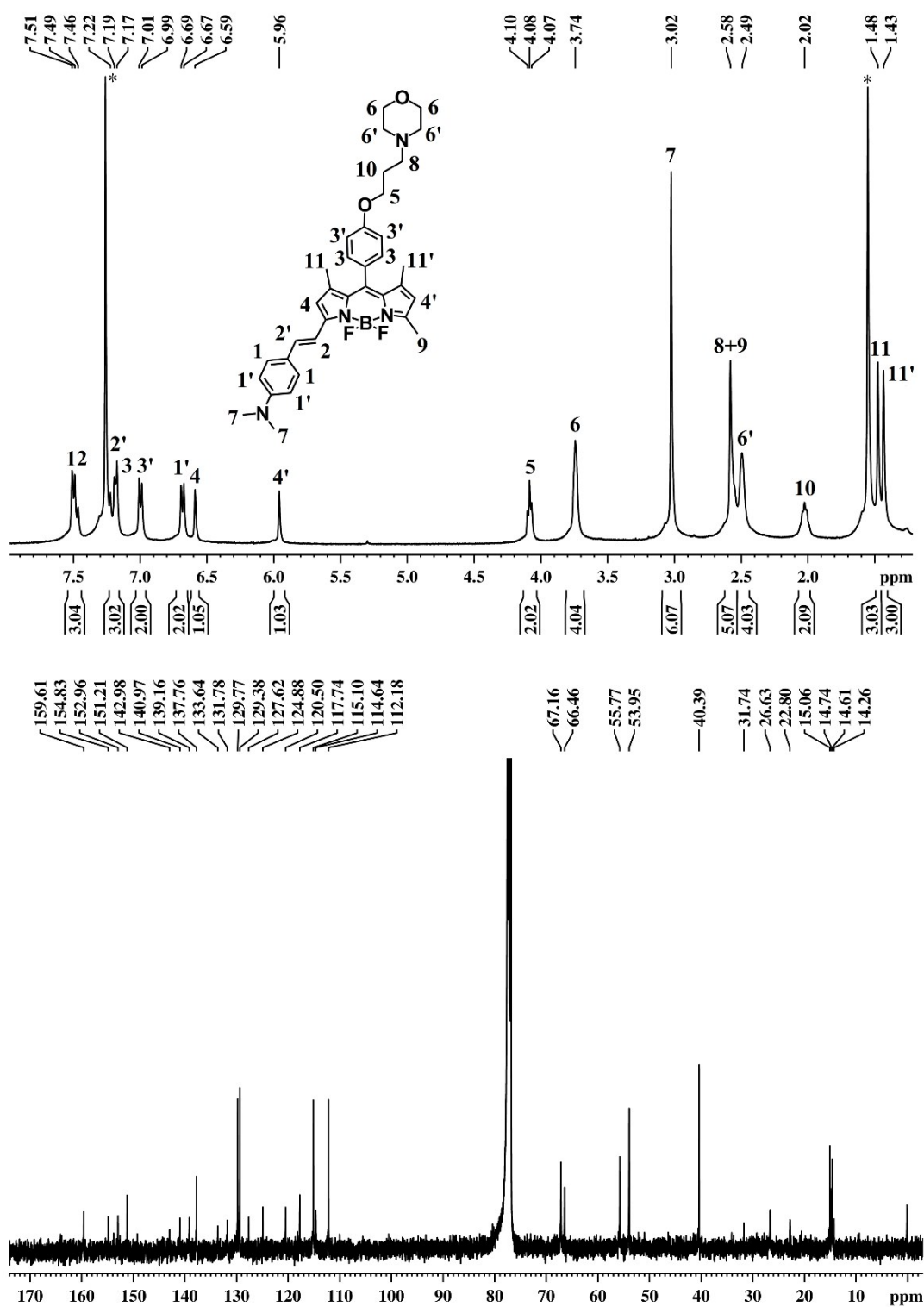


Fig. S1 ¹H NMR and ¹³C NMR spectra of probe A in CDCl₃ at 293 K. * indicate the residual solvent and H₂O signals.

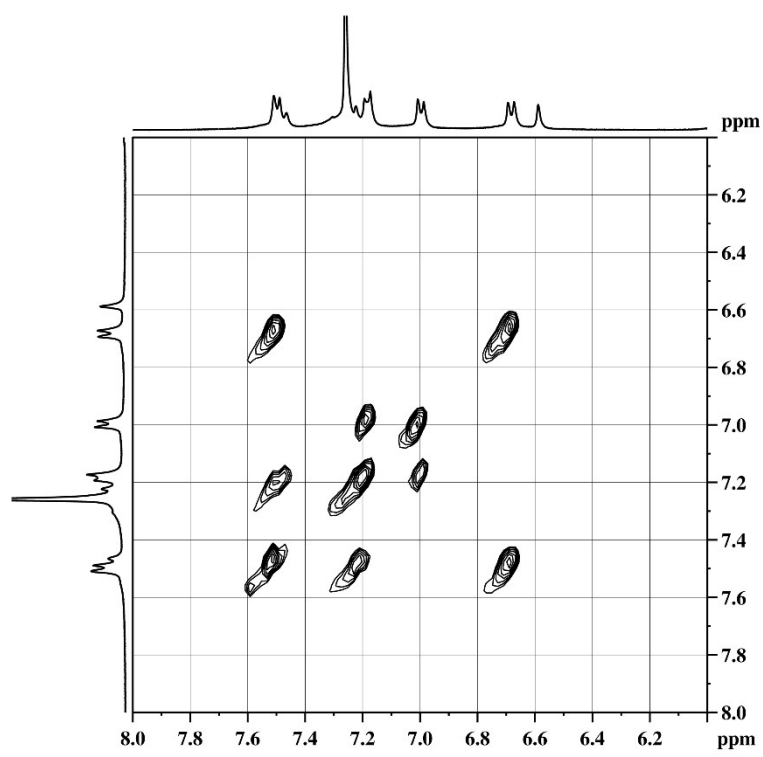
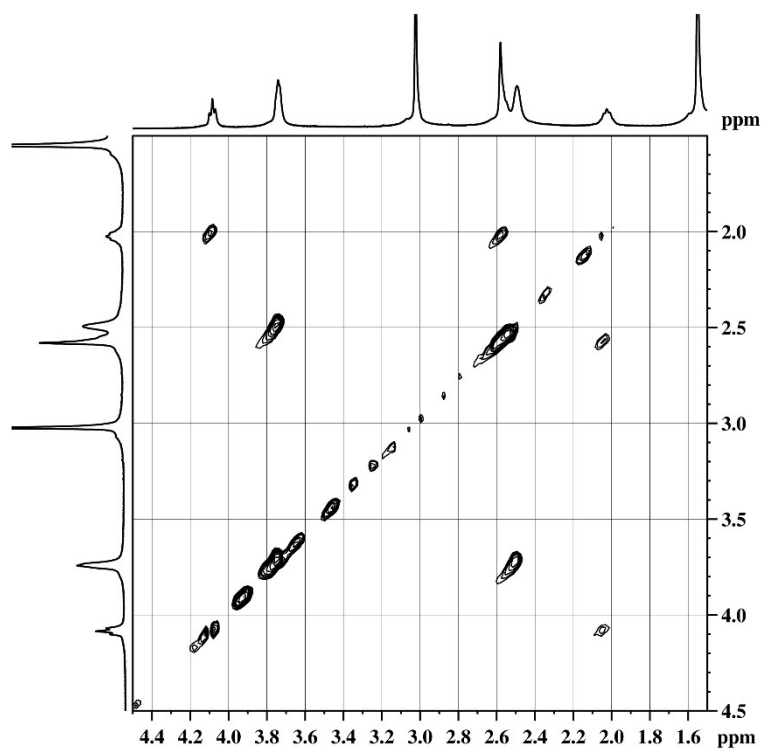


Fig. S2 ¹H-¹H COSY spectra of probe A in CDCl₃ at 293 K.

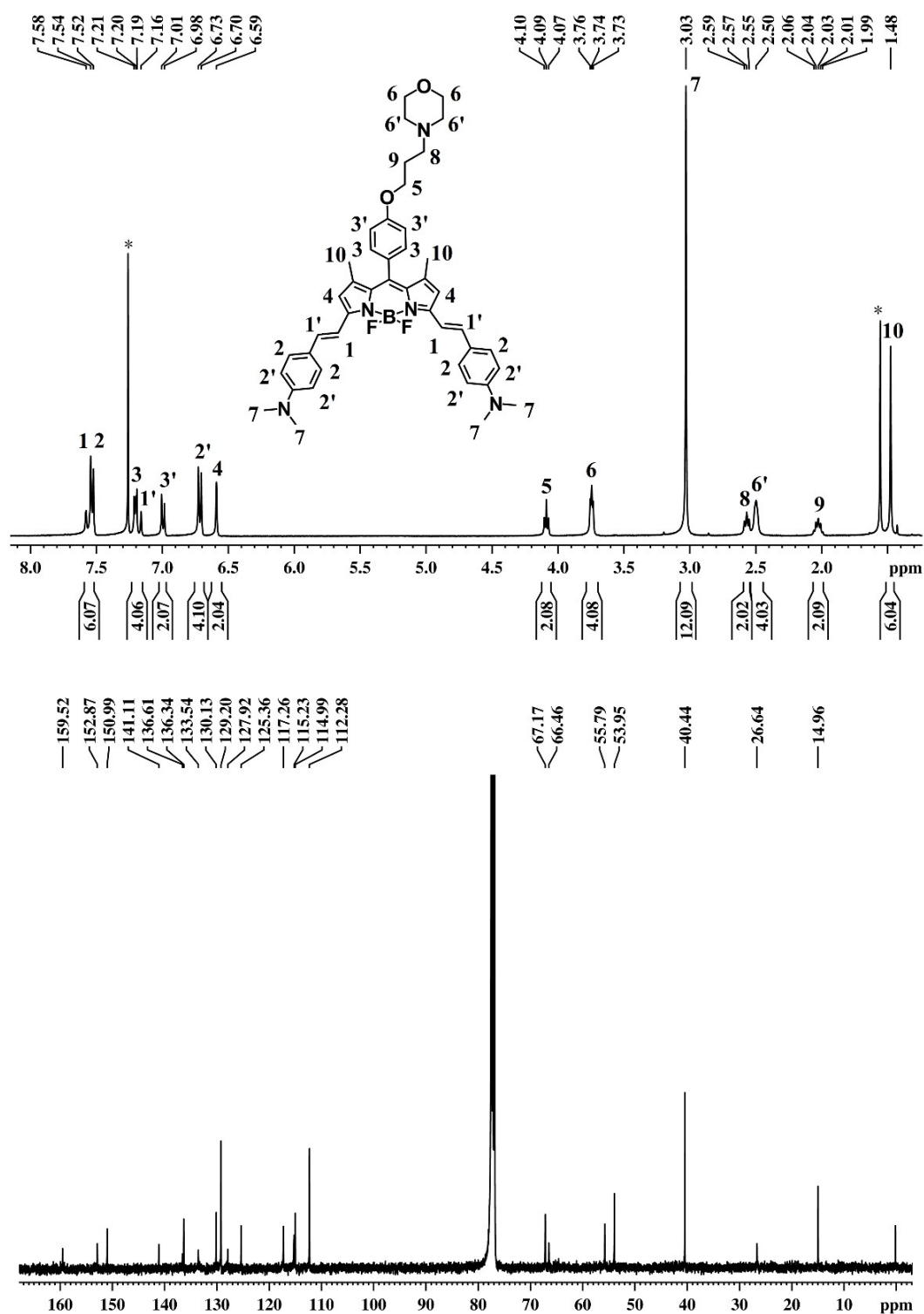


Fig. S3 ^1H NMR and ^{13}C NMR spectra of probe **B** in CDCl_3 at 293 K. * indicate the residual solvent and H_2O signals.

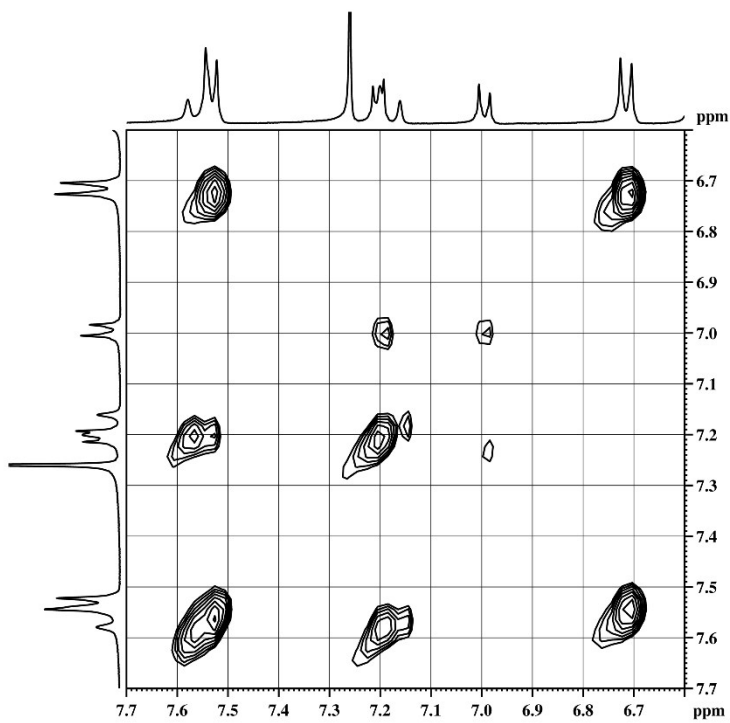
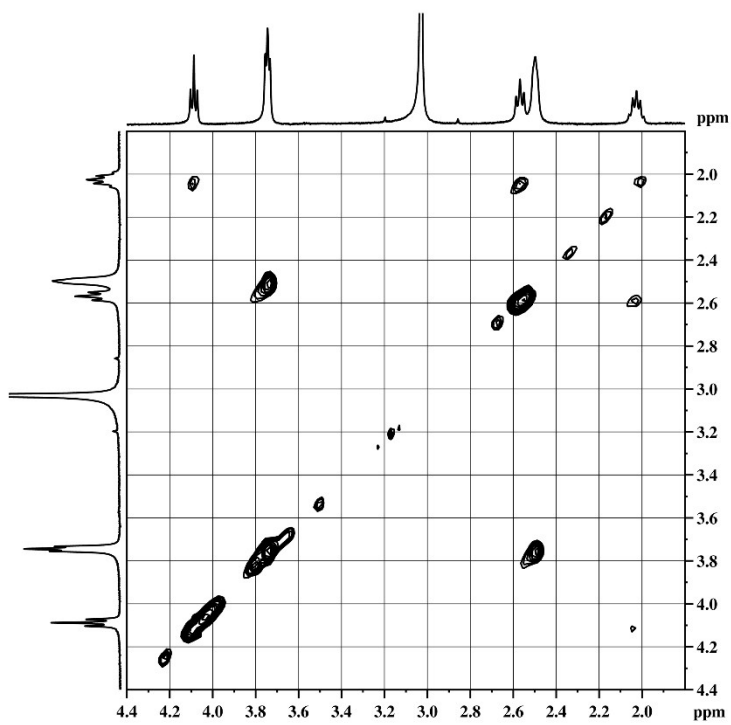


Fig. S4 ^1H - ^1H COSY spectra of probe **B** in CDCl_3 at 293 K.

Table S1 Photophysical properties of **A** and **B** in several solvents.

solvent	λ_{abs} (max/nm)	$\log \epsilon_{\text{max}}$	λ_{em} (max/nm)	$\Delta\nu_{\text{max}}$ (nm)	$\Phi_{\text{f}}^{\text{a}}$
Toluene	607	5.07	641	34	0.84
CHCl ₃	605	5.02	650	45	0.59
A THF	600	5.03	652	52	0.38
Acetone	597	5.03	664	67	0.13
CH ₃ CN	596	5.01	674	78	0.03
Toluene	699	5.13	724	25	0.08
CHCl ₃	697	5.08	726	29	0.05
B THF	692	5.10	729	37	0.05
Acetone	692	5.08	730	38	0.02
CH ₃ CN	691	5.04	731	40	0.01

^a Fluorescence quantum yields were determined by reference to H₂TPP in benzene ($\Phi = 0.13$).²

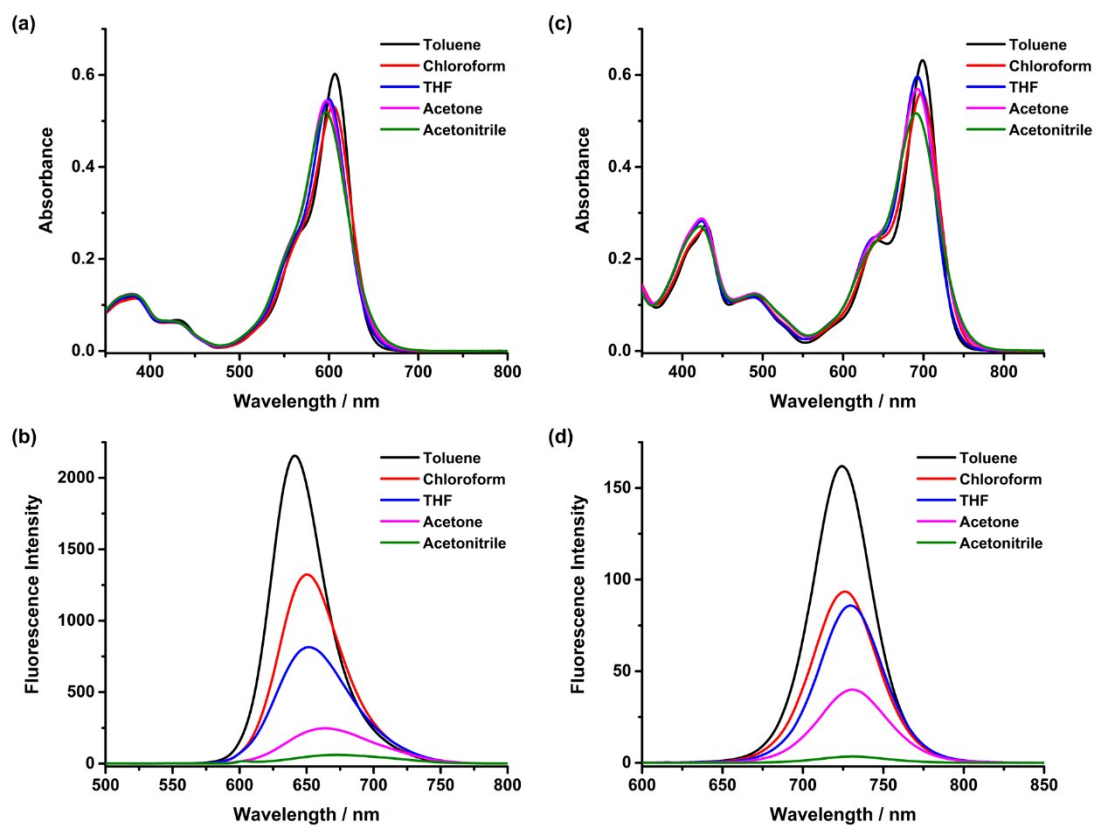


Fig. S6 (a) Absorption spectra of **A** (5 μM) in different solvents and (b) the corresponding emission spectra of **A** ($\lambda_{\text{ex}} = 600$ nm); (c) Absorption spectra of **B** (5 μM) in different solvents and (d) the corresponding emission spectra of **B** ($\lambda_{\text{ex}} = 700$ nm).

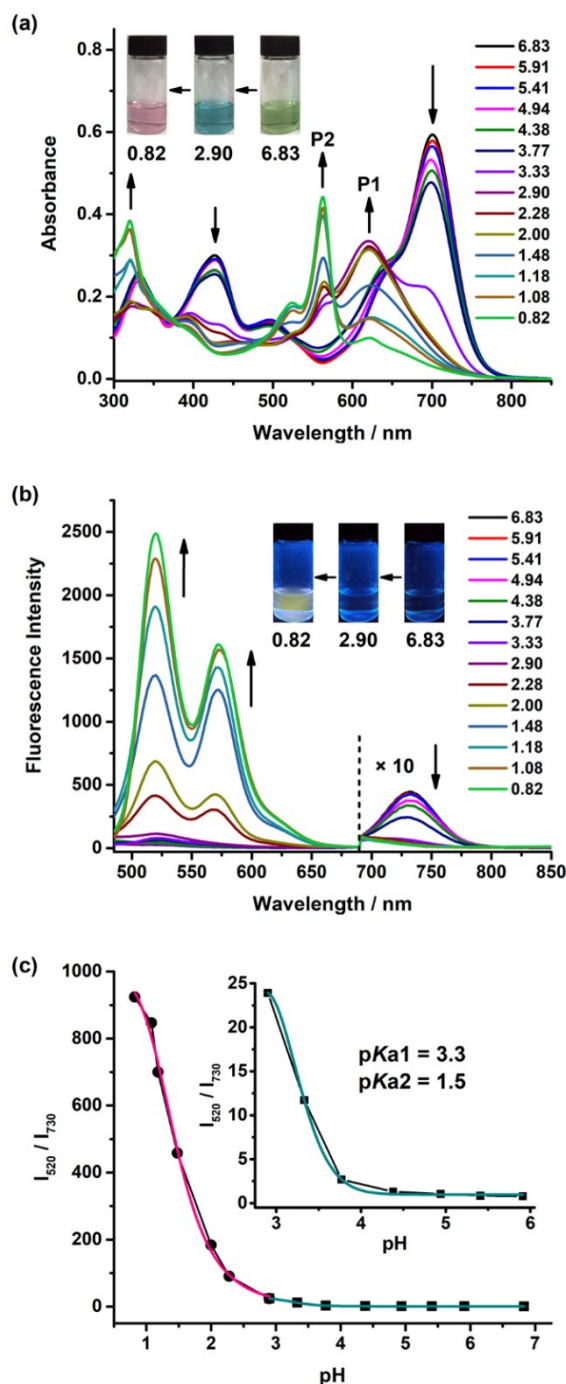


Fig. S7 Optical responses of probe **B** (5 μM) in THF/H₂O (1:1, v/v) at different pH values. (a) Absorption spectra. Inset: photographs at pH 0.82, 2.90 and 6.83 under natural light. (b) Emission spectra ($\lambda_{\text{ex}} = 480 \text{ nm}$). Inset: photographs at pH 0.82, 2.90 and 6.83 under 365 nm irradiation. (c) Fluorescence intensity ratios I_{520}/I_{730} at pH 6.83-0.82. Inset: Fluorescence intensity ratio versus pH values in the pH range of 5.91-2.90.

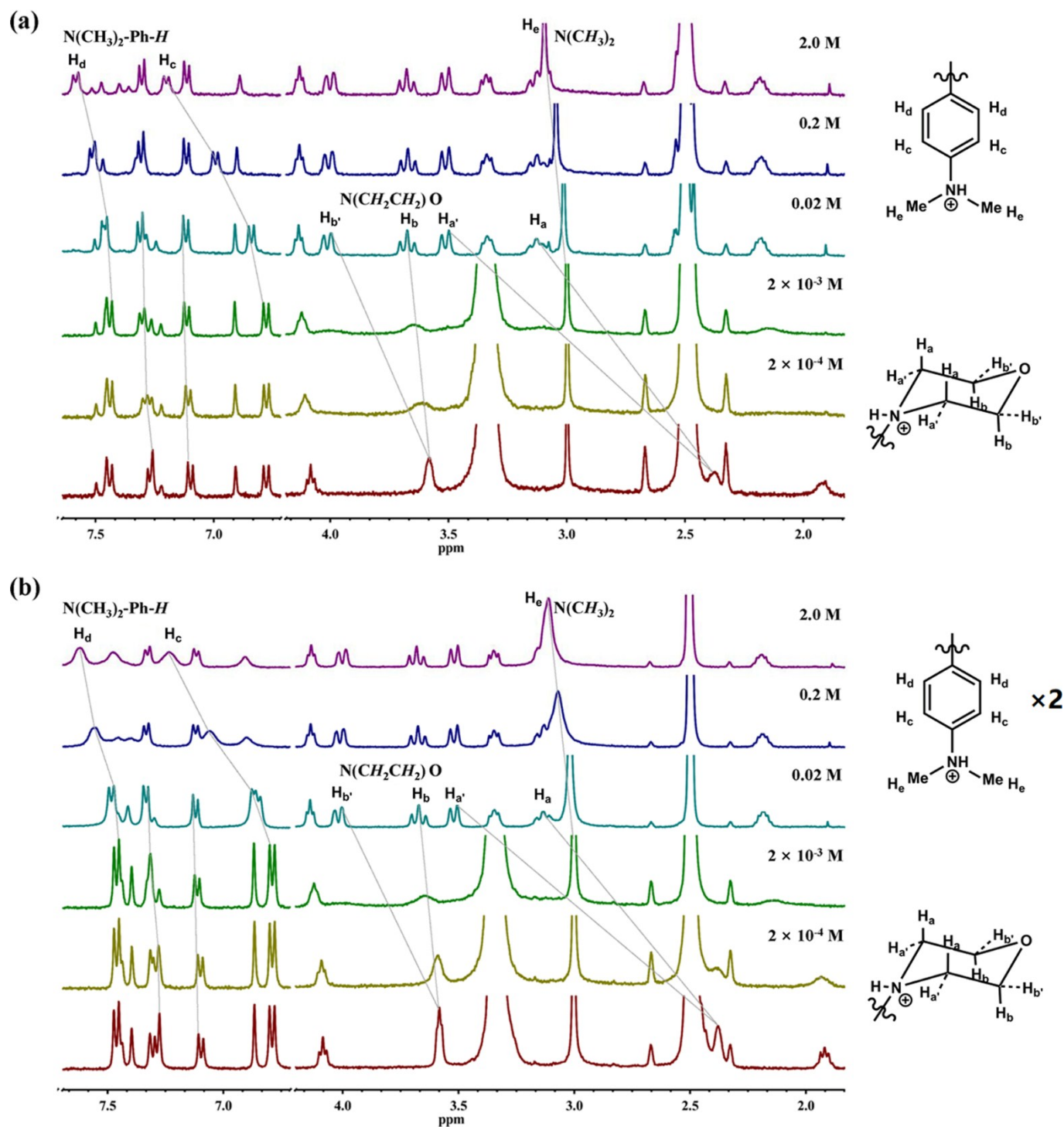


Fig. S8 ^1H NMR spectra of probes A (a) and B (b) in 0.5 mL of $\text{DMSO-}d_6$ after addition of CF_3COOD (0 - 2.0 M).

Theoretical Calculations.

The energy levels of the highest occupied molecular orbital (HOMO) and lowest unoccupied molecular orbital (LUMO) were determined by the density functional theory (DFT) calculations carried out by B3LYP-D3(0) method with 6-311G(d) basis set.³⁻⁵ Besides, tetrahydrofuran was used to simulate the mixed solution environment with the solvation model based on density (SMD).⁶ All the calculations were carried out by *Gaussian 09* program.⁷

Table S2 The frontier molecular orbital energy levels (in eV) of **A**, **AP**, **B**, **BP1**, **BP2**, morpholine moiety (N-methylmorpholine) and protonated morpholine moiety (protonated N-methylmorpholine).

	A	AP	B	BP1	BP2	morpholine	morpholine + H ⁺
LUMO	-2.58	-3.19	-2.59	-3.13	-3.57	1.22	-0.17
HOMO	-4.84	-5.78	-4.55	-5.14	-5.84	-5.80	-8.06
Gap	2.26	2.58	1.96	2.00	2.26	7.02	7.89

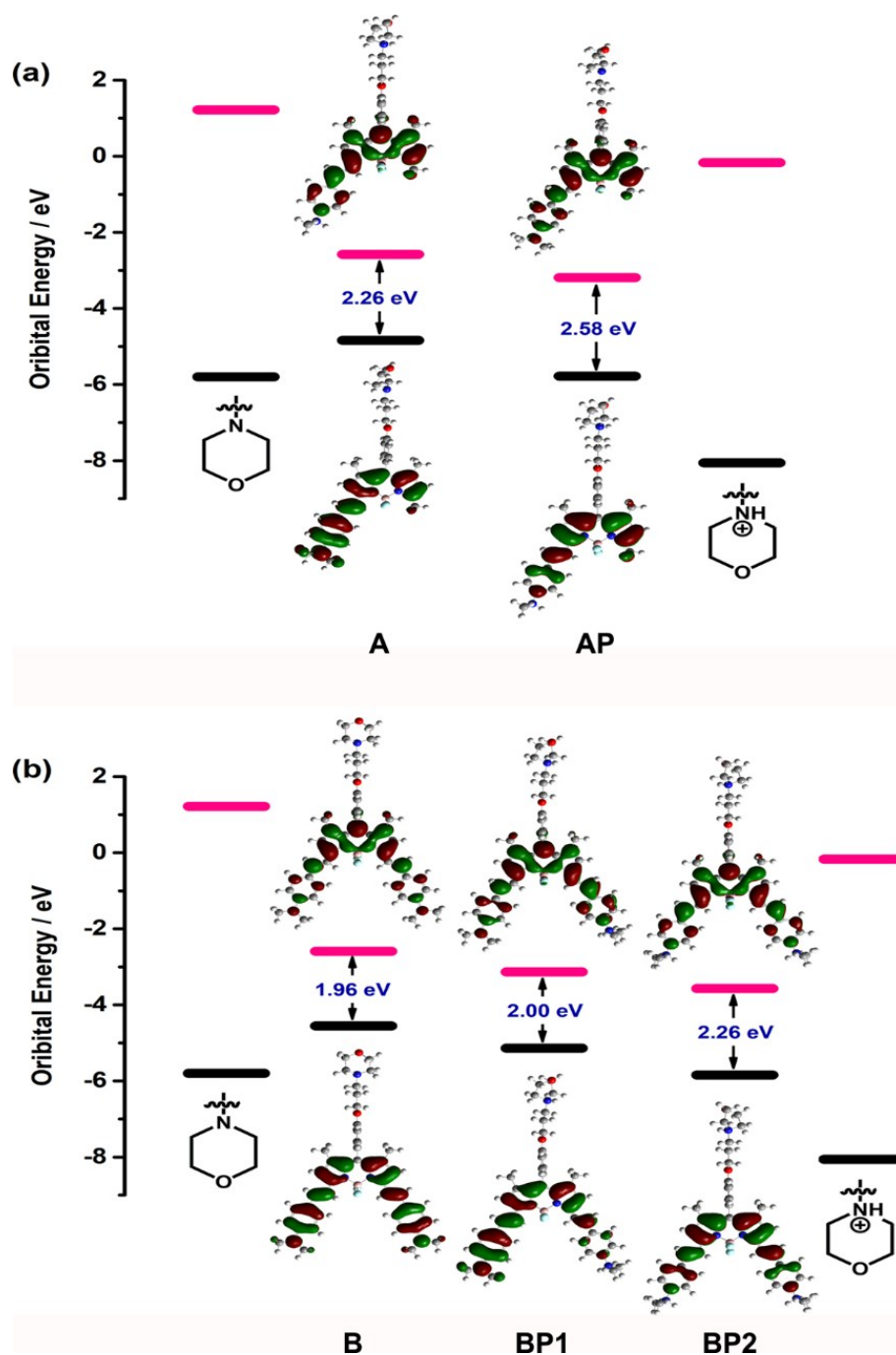
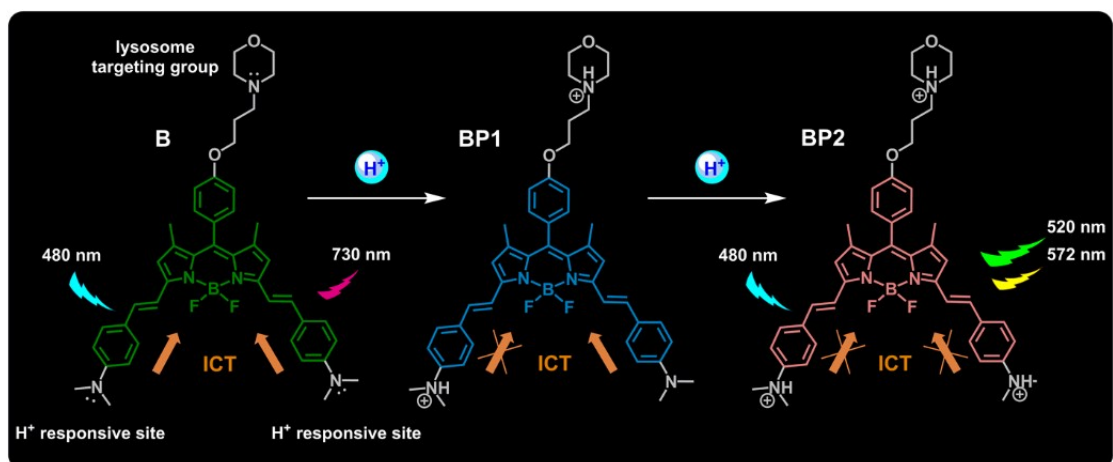


Fig. S9 (a) HOMO and LUMO energy levels and of **A**, **AP**, morpholine moiety and protonated morpholine moiety, as well as the electron density distributions in HOMO and LUMO of **A** and **AP**; (b) HOMO and LUMO energy levels of **B**, **BP1**, **BP2**, morpholine moiety and protonated morpholine moiety, as well as the electron density distributions in HOMO and LUMO of **B**, **BP1**, and **BP2**.



Scheme S2 The pH-modulated ICT mechanism for probe **B**.

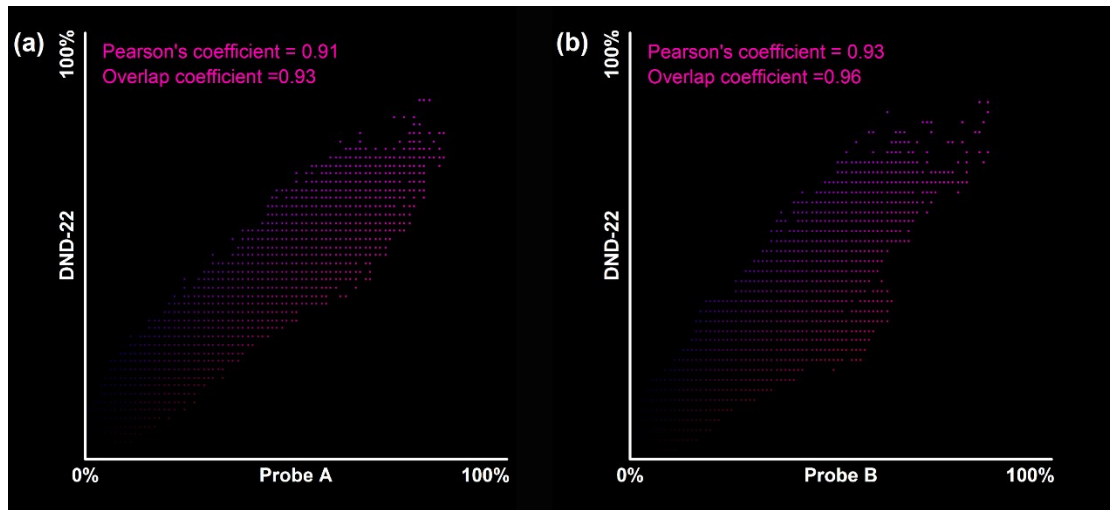


Fig. S10 (a) The correlation of probe **A** (red channel) and LysoTracker™ Blue DND-22 (blue channel). (b) The correlation of probe **B** (deep red channel) and LysoTracker™ Blue DND-22 (blue channel).

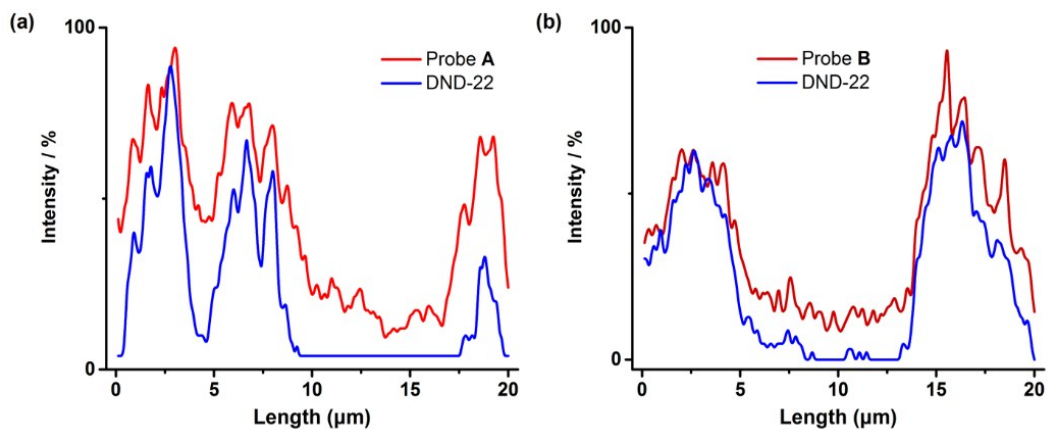


Fig. S11 (a) Intensity profiles within the ROI (orange lines in **Fig. 2a**) of probe **A** and DND-22 across A549 cells. (b) Intensity profiles within the ROI (orange lines in **Fig. 2b**) of probe **B** and DND-22 across A549 cells.

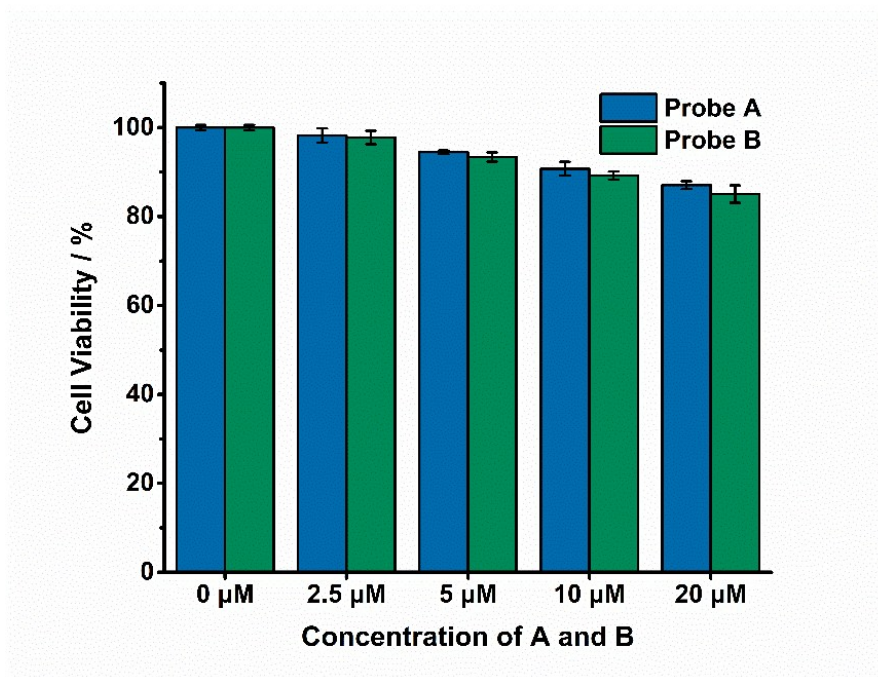


Fig. S12 Cell viability (%) estimated by a MTT assay versus incubation in different concentration of **A** and **B** (2.5 - 20 μM).

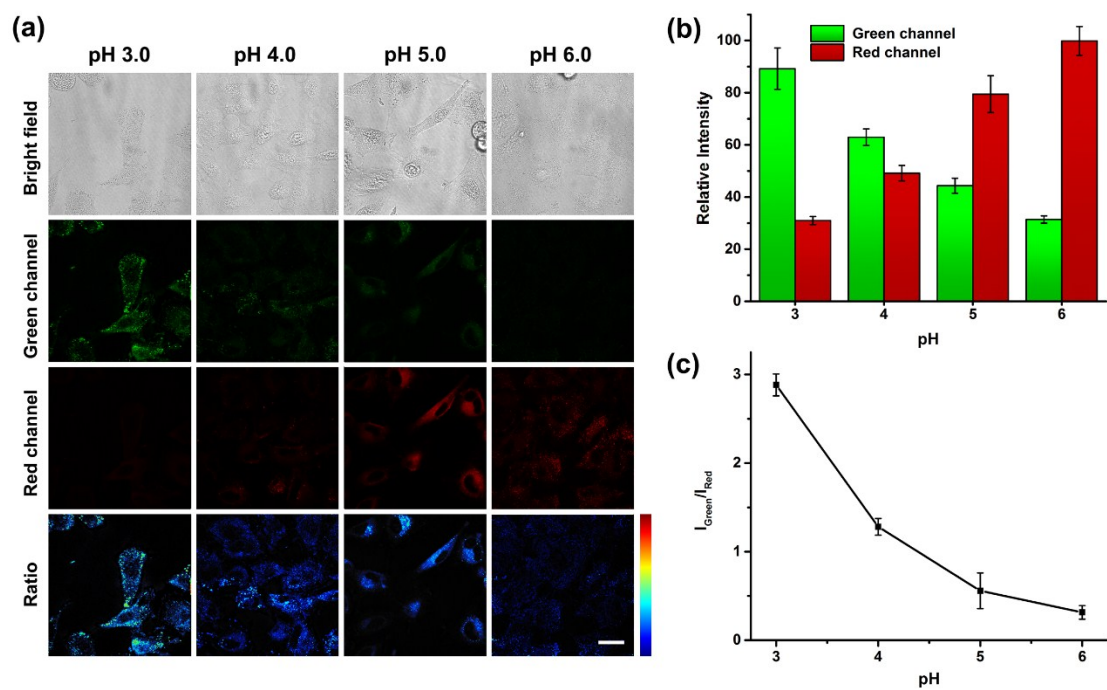


Fig. S13 (a) Fluorescence images for probe **B** (5 μM) in A549 cells at various pH: green channel ($\lambda_{\text{em}} = 515\text{-}565$ nm), deep red channel ($\lambda_{\text{em}} = 675\text{-}725$ nm), $\lambda_{\text{ex}} = 488$ nm. Ratio images represent the ratio of fluorescence intensity between green channel and red channel ($I_{\text{green}}/I_{\text{red}}$). (b) Quantified relative fluorescence intensity at various pH. (c) Ratio of $I_{\text{green}}/I_{\text{red}}$ at various pH. Scale bars = 20 μm.

References

1. A. Coskun, E. Deniz and E. U. Akkaya, *Org. Lett.*, 2005, **7**, 5187-5189.
2. D. J. Quimby and F. R. Longo, *J. Am. Chem. Soc.*, 1975, **97**, 5111-5117.
3. R. Krishnan, J. S. Binkley, R. Seeger and J. A. Pople, *J. Chem. Phys.*, 1980, **72**, 650-654.
4. P. J. Stephens, F. J. Devlin, C. F. Chabalowski and M. J. Frisch, *J. Chem. Phys.*, 1994, **98**, 11623-11627.
5. S. Grimme, J. Antony, S. Ehrlich and H. Krieg, *J. Chem. Phys.*, 2010, **132**, 154104.
6. A. V. Marenich, C. J. Cramer and D. G. Truhlar, *J. Phys. Chem. B*, 2009, **113**, 6378-6396.
7. M. J. Frisch, G. W. Trucks, H. B. Schlegel, G. E. Scuseria, M. A. Robb, J. R. Cheeseman, G. Scalmani, V. Barone, G. A. Petersson, H. Nakatsuji, X. Li, M. Caricato, A. V. Marenich, J. Bloino, B. G. Janesko, R. Gomperts, B. Mennucci, H. P. Hratchian, J. V. Ortiz, A. F. Izmaylov, J. L. Sonnenberg, Williams, F. Ding, F. Lipparini, F. Egidi, J. Goings, B. Peng, A. Petrone, T. Henderson, D. Ranasinghe, V. G. Zakrzewski, J. Gao, N. Rega, G. Zheng, W. Liang, M. Hada, M. Ehara, K. Toyota, R. Fukuda, J. Hasegawa, M. Ishida, T. Nakajima, Y. Honda, O. Kitao, H. Nakai, T. Vreven, K. Throssell, J. A. Montgomery Jr., J. E. Peralta, F. Ogliaro, M. J. Bearpark, J. J. Heyd, E. N. Brothers, K. N. Kudin, V. N. Staroverov, T. A. Keith, R. Kobayashi, J. Normand, K. Raghavachari, A. P. Rendell, J. C. Burant, S. S. Iyengar, J. Tomasi, M. Cossi, J. M. Millam, M. Klene, C. Adamo, R. Cammi, J. W. Ochterski, R. L. Martin, K. Morokuma, O. Farkas, J. B. Foresman and D. J. Fox, Wallingford, CT, 2016.